Effects of some parameters on numerical simulation of coastal bed morphology

Dang Huu Chung
Institute of Mechanics, Vietnamese Academy of Science and Technology, Hanoi, Vietnam, and
Dieter P. Eppel
Institute for Coastal Research, GKSS Research Centre, Geesthacht, Germany

Received 10 January 2006
Revised 21 May 2007
Accepted 7 June 2007

Abstract

Purpose – The aim is to investigate in detail the sensitivity of sediment transport and bed morphology with respect to some parameters including bed slope, non-hydrostatic pressure term, sand grain size, temperature, salinity and lower boundary conditions for suspended sand concentration on a regional scale through numerical simulations based on a mathematical model.

Design/methodology/approach – The numerical model consists of a 3D hydrodynamic code amended by a sediment transport module. At the same time, the influence of wave action has been taken into account. The model is applied to the Sylt-Romo tidal bay covering approximately $20 \times 30\,km^2$ spanned by about 2.7×10^6 active grid points with the constant wind and wave fields.

Findings – The computed results of seven different cases over 150 h show that the effect of bed slope correction is very strong, especially in case of largely changeable bathymetry and depends on the horizontal grid resolution. Sand grain size strongly influences the vertical distribution of suspended sediment and then sedimentation. The impact of sea water temperature is relatively clear despite being less powerful than two former parameters. Non-hydrostatic pressure perturbations of the flow field and the kind of the lower boundary condition as well as salinity are negligible allowing for considerable savings of CPU time when the numerical simulation is carried out for a large area and for a very long-time period.

Originality/value – The results of the study demonstrate that the geometrical factor of coastal bed and the range of sand particle size on the bottom contribute to the tendency of bed evolution in some measure. Additionally, the increase of temperature of sea water due to global warming may also make a considerable change to the mechanism of sediment transport and sedimentation in future. Therefore, the human intervention in the process of natural evolution is possible through the behaviour to the nature. At the same time, this is also interesting and useful information and it can consolidate the idea for coastal engineering projects.

Keywords Modelling, Numerical analysis, Sedimentation, Coastal regions, Hydrodynamics

Paper type Research paper

Nomenclature

c	= sand concentration	c_{max}	= maximum computed sand concentration after 150 h
c_a	= sand concentration at reference level	d_{50}	= median grain diameter

This paper is a part of works carried out in the frame of the Scholarship Program of GKSS Research Centre, Institute for Coastal Research. The first author would like to express his deep gratitude to Dr Dieter Eppel and Dr Rolf Riethmueller for their heartfelt help during his stay in Germany.

International Journal of Numerical Methods for Heat & Fluid Flow
Vol. 18 No. 5, 2008
pp. 575-592

0961-5539
DOI 10.1108/09615530810879729

D_* = dimensionless grain size
g = gravity
G = solution domain
h = water depth
i, j, k = Grid point subscripts
L = land boundary of solution domain
m, n = parameters in bed load formula
$\vec{n}$ = normal unit vector on L
p_r = porosity
p' = non-hydrostatic pressure correction
q_b = bed load transport
$q_{t\max}$ = maximum total sediment flux after 150 h
q_{tx}, q_{ty} = total sediment flux components
s = ratio of sand density and water density
t = time
T_s = transport parameter
$\vec{U}$ = depth-averaged velocity vector
$\vec{V}$ = $(u, v, w)^T$, velocity vector of flow
$V_{\max}$ = maximum velocity of flow after 150 h
$\vec{V}_s$ = $(u, v, w - w_s)^T$
w_s = settling velocity of sand particle
x, y, z = Cartesian coordinates
z_a = suspended sediment reference level
z_b = bed level
z_{bi} = bed level of case i ($i = 1/7$) after 150 h
Γ = lateral open boundary of solution domain
Δ_s = height of sand wave
Δz_{bdm} = mean deposition level after 150 h
Δz_{bem} = mean erosion level after 150 h
Δz_{bm1} = mean bed-level change after 150 h for Case 1
Δ = $z_{b1} - z_{bi}$, ($i = 2/7$) after 150 h
Δ_m = mean value of $|\Delta|$
$\alpha_k, \beta_k, \delta_k$ = coefficients in difference equations
η = water level
ν^h, ν^v = horizontal and vertical momentum diffusion coefficients
$\varepsilon_s^h, \varepsilon_s^v$ = horizontal and vertical diffusion coefficients for suspended sediment
ρ_0 = constant water density
ρ_s = sediment density
ρ' = deviation from constant water density
τ = bed shear stress
τ_{0s} = bed shear stress due to skin friction
τ_{cr} = critical bed shear stress
θ = dimensionless bed shear stress
θ_{cr} = critical dimensionless bed shear stress
θ_{cr0} = critical dimensionless bed shear stress for flat bed
ϕ_r = angle of repose
φ = parameter in bed load formula
$\vec{\Omega}$ = $(fv, -fu, 0)^T$, Coriolis acceleration vector
∇ = $((\partial/\partial x), (\partial/\partial y), (\partial/\partial z))^T$
∇_{xy} = $((\partial/\partial x), (\partial/\partial y), 0)^T$

Introduction

Coastal zone management and sea defence planning increasingly rely on numerical models when information is needed on the hydrodynamic state of a coastal section measured and its changes by erosion and deposition, be they occurring naturally or triggered by engineering work. Though 3D models for free-surface flow, amended by equations for sediment transport and bottom evolution, are still subject of ongoing research, the increase in computer power brings these models within the reach of real-world applications.

In fact, there were many similar studies before, in which the effects of some physical parameters were investigated through a 3D numerical model, such as the effect of thermal expansion from the comparison of computed results for Boussinesq and non-Boussinesq approximations (Mellor and Ezer, 1995) or the studies on sensitivity of ocean mean state and variability to kinds of boundary condition, the resolution of computational grid and the different choices of diffusion and viscosity (Ezer and Mellor, 2000), etc.

In this paper, the behaviour of a sediment transport parameterization and the sensitivities of bed morphodynamics are investigated within the context of a numerical 3D hydrodynamical model. It is to be expected that changes in bed morphology due to erosion and deposition will affect the dynamics during storm events and will change the long-term structure of the flow. Short-term simulations of the bottom evolution of the Sylt-Romo tidal bay under the influence of strong wind and tidal water motion for the period from 23 May 1992 to 30 May 1992 are presented. The aim is to assess the sensitivity of the calculated bed change on some parameters affecting the sediment transport in a close-to-realistic setting. Although the quantitative differences in bed level changes are small over the few days simulated for the different choices of parameters, it is to be expected that, in long-term simulations, these effects can be dramatic. Simulations have been performed for different lower boundary conditions imposed on the suspended-sediment concentration for different grain sizes. In addition, bed slope effects have been investigated as well as the influence of the pressure approximation in the momentum equations (hydrostatic vs non-hydrostatic) on sediment transport. The effects of temperature and salinity are also important and had been studied already in Dang Huu (2007) on the basis of 1DV model. Once again, they are also included in this study but within a 3D model and to be evaluated together the other parameters. Although the parameters mentioned above are not a complete set reflecting the very complicated process of coastal bed morphodynamics and depend on different methods of parameterization, but at least their roles and importance are shown scientifically within a numerical model.

The period over which sediment transport was simulated is characterized by windy weather with maximum wind speeds of about 17 m/s coming from north-west direction. The wave field was also taken into account and supposed to propagate in the same direction of wind with a constant height of 0.5 m. These assumptions were used as an alternative solution for the lack of measured data. This problem itself makes the predicted results become less convinced. However, it is acceptable for the evaluations trending towards qualitative study.

Model equations

The simulation model is based on the Reynolds-averaged Navier-Stokes equations for an incompressible free-surface flow with the non-hydrostatic pressure correction included, together with the transport equation for suspended sediment concentration and an equation describing the bottom evolution:

$$\nabla \cdot \vec{V} = 0 \tag{1}$$

$$\frac{\partial \vec{V}}{\partial t} + (\nabla \cdot \vec{V})\vec{V} = -g\nabla\eta - \frac{g}{\rho_0}\int_z^\eta \nabla_{xy}\rho' dz' - \nabla p' + \nu^{\mathrm{h}}\nabla_{xy}^2\vec{V} + \frac{\partial}{\partial z}\left(\nu^{\mathrm{v}}\frac{\partial \vec{V}}{\partial z}\right) + \vec{\Omega} \tag{2}$$

$$\frac{\partial c}{\partial t} + \vec{V}_{\mathrm{s}} \cdot \nabla c = \varepsilon_{\mathrm{s}}^{\mathrm{h}}\nabla_{xy}^2 c + \frac{\partial}{\partial z}\left(\varepsilon_{\mathrm{s}}^{\mathrm{v}}\frac{\partial c}{\partial z}\right) \tag{3}$$

$$\frac{\partial z_{\mathrm{b}}}{\partial t} - \frac{1}{1-p_{\mathrm{r}}}\left(\frac{\partial q_{tx}}{\partial x} + \frac{\partial q_{ty}}{\partial y}\right) = 0 \tag{4}$$

In order to close the system of equations, the following initial and boundary conditions are used:

$$\eta(x,y,z,t)=0, \vec{V}(x,y,z,t)=0, t=0, \quad \forall (x,y,z)\in G \tag{5}$$

$$c(x,y,z,t)=0, z_{\mathrm{b}}(x,y,t)=f_1(x,y), t=0, \quad \forall (x,y,z)\in G \tag{6}$$

$$\vec{V}\cdot\vec{n}=0, \quad \forall (x,y,z)\in L, \quad \forall t\geq 0 \tag{7}$$

$$c(x,y,z,t)=f_2(x,y,z,t), \quad \forall (x,y,z)\in \Gamma, \quad \forall t\geq 0 \tag{8}$$

$$-\varepsilon_{\mathrm{s}}^{\mathrm{v}}\frac{\partial c}{\partial z}=w_{\mathrm{s}}c, \quad \forall (x,y,z)\in G, z=\eta, \quad \forall t\geq 0, \tag{9}$$

in which $f_i\,(i=1,2)$ = linear interpolation functions from measured data. The function f_2 is set to zero assuming no concentration at the open boundary.

Simulations with two different choices for the lower boundary values of the suspended sediment concentration were performed (see Dang Huu and van Rijn, 2003 for a similar setup). In the first case, the mixed boundary condition is applied, e.g. when erosion occurs, a reference concentration, c_a, at the interface layer z_a separating suspended sediment and bedload transport was prescribed as a Dirichlet boundary condition:

$$c(x,y,z,t)=c_a(x,y,t), \quad \forall (x,y,z)\in G,\ z=-z_{\mathrm{b}}+z_a, \quad \forall t\geq 0, \tau>\tau_{\mathrm{cr}} \tag{10}$$

And when deposition occurs, the Neumann boundary condition is applied:

$$-\varepsilon_{\mathrm{s}}^{\mathrm{v}}\frac{\partial c}{\partial z}=w_{\mathrm{s}}c, \quad \forall (x,y,z)\in G,\ z=-z_{\mathrm{b}}+z_a, \quad \forall t\geq 0, \tau\leq\tau_{\mathrm{cr}} \tag{11}$$

In the second case, the Dirichlet boundary condition only, equation (10), is used.

It should be noted that the horizontal and vertical eddy viscosity coefficients as well as the diffusion coefficients for suspended sediment obtain the constant value of 10^{-5} for simplicity.

Numerical integration of the additional equations

The system of equations (1)-(4) are numerically solved at the same time with finite difference method, in which the hydrodynamical equations for the unknown variables of water level and velocity components (equations (1)-(2)) are solved by operator splitting of the finite-difference equations combining a semi-Lagrangean treatment of the advective terms with a semi-implicit discretization of the vertical diffusion terms. The discretized equations are five or seven-diagonal system and are iteratively solved with a very effective conjugate gradient method. The algorithm of this part is described in more detail in Casulli and Cattani (1994) Casulli and Stelling (1998) and Kapitza (2001).

The additional equation for suspended-sediment transport, equation (3), is integrated with similar techniques as used in Casulli's model. Introducing characteristics:

$$\frac{\mathrm{d}x}{\mathrm{d}t}=u, \frac{\mathrm{d}y}{\mathrm{d}t}=v, \frac{\mathrm{d}z}{\mathrm{d}t}=w-w_{\mathrm{s}}, \tag{12}$$

equation (3) then becomes:

$$\frac{\mathrm{d}c}{\mathrm{d}t}=\frac{\partial}{\partial x}\left(\varepsilon_{\mathrm{s}}^{\mathrm{h}}\frac{\partial c}{\partial x}\right)+\frac{\partial}{\partial y}\left(\varepsilon_{\mathrm{s}}^{\mathrm{h}}\frac{\partial c}{\partial y}\right)+\frac{\partial}{\partial z}\left(\varepsilon_{\mathrm{s}}^{\mathrm{v}}\frac{\partial c}{\partial z}\right), \tag{13}$$

equation (13) is solved by operator splitting. First, equation (12) is integrated to determine the inter-grid position $(i-d, j-e, k-f)$ on the characteristics by

backward time difference scheme, and then the value of concentration at this position is calculated by trilinear interpolation:

$$\tilde{c}_{ijk} = c^{n}_{i-d,j-e,k-f} \tag{14}$$

equation (13) is discretized on the characteristics with only the vertical diffusion term taken at a time level $n+1$:

$$\begin{aligned} c^{n+1}_{ijk} = \tilde{c}_{ijk} &+ \Delta t\left\{\frac{\partial}{\partial x}\left(\varepsilon^{\mathrm{h}}_{\mathrm{s}}\frac{\partial c}{\partial x}\right) + \frac{\partial}{\partial y}\left(\varepsilon^{\mathrm{h}}_{\mathrm{s}}\frac{\partial c}{\partial y}\right)\right\}^{n}_{i-d,j-e,k-f} \\ &+ \Delta t\left\{\frac{\partial}{\partial z}\left(\varepsilon^{\mathrm{v}}_{\mathrm{s}}\frac{\partial c}{\partial z}\right)\right\}^{n+1}_{ijk}, \end{aligned} \tag{15}$$

finally, discretizing the diffusion operator by central differences leads to a tridiagonal equation system for a box in layer k:

$$\alpha_k c^{n+1}_{ijk} + \beta_k c^{n+1}_{ijk} + \gamma_k c^{n+1}_{ijk} = \delta_k, \quad (i = 2, i_{\max} - 1, j = 2, j_{\max} - 1, k = 2, k_{\max -1}) \tag{16}$$

where:

$$\gamma_k = -\frac{\Delta t \varepsilon^{\mathrm{v}}_{sk-1/2}}{\Delta z_{tk-1}}, \alpha_k = \gamma_{k+1}, \beta_k = \Delta z_{ck} - \gamma_{k+1} - \gamma_k, \delta_k = F^{n}_{ijk}\Delta z_{ck}$$

$$\Delta z_{ck} = h_k - h_{k+1}, \Delta z_{tk} = 0.5\left(\Delta z_{ck} + \Delta z_{ck+1}\right)$$

$$F^{n}_{ijk} = \tilde{c}_{ijk} + \Delta t\left\{\frac{\partial}{\partial x}\left(\varepsilon^{\mathrm{h}}_{\mathrm{s}}\frac{\partial c}{\partial x}\right) + \frac{\partial}{\partial y}\left(\varepsilon^{\mathrm{h}}_{\mathrm{s}}\frac{\partial c}{\partial y}\right)\right\}^{n}_{i-d,j-e,k-f}.$$

The advection-diffusion operators occurring in the other equations are discretized in the same manner and solved by the Thomas algorithm.

The second order Lax-Wendroff scheme is used to update the bottom evolution equation (4) assuming q_{tx}, q_{ty} to be proportional to the depth averaged velocity, U, or via water flux, Q with a proportional constant A:

$$q_{tx,y} = AU^{\alpha} = A\left(\frac{Q}{z_{\mathrm{b}}}\right)^{\alpha}, \tag{17}$$

and then:

$$\frac{\partial q_{tx,y}}{\partial z_{\mathrm{b}}} = -\frac{\alpha q_{tx,y}}{z_{\mathrm{b}}}, \tag{18}$$

in which $\alpha = 2$ (Chesher *et al.*, 1993). Hence:

$$\begin{aligned} \Delta z_{\mathrm{b}ij} &\equiv z^{n+1}_{\mathrm{b}ij} - z^{n}_{\mathrm{b}ij} \\ &= \Delta t R^{n}_{ij} - \frac{1}{2}\Delta t^2\left\{\frac{(Q_x R)^{n}_{i+1j} - (Q_x)^{n}_{i-1j}}{2\Delta x} + \frac{(Q_y R)^{n}_{ij+1} - (Q_y)^{n}_{ij-1}}{2\Delta y}\right\}, \\ &\left(i = 2, i_{\max} - 1, j = 2, j_{\max} - 1, n = 0, n_{\max} - 1\right), \end{aligned} \tag{19}$$

with:

$$Q^n_{xij} = \frac{\alpha q^n_{txij}}{(1-p_r)z^n_{bij}}, Q^n_{yij} = \frac{\alpha q^n_{tyij}}{(1-p_r)z^n_{bij}}$$

$$R^n_{ij} = \frac{1}{1-p_r}\left\{\frac{q^n_{txi+1/2j} - q^n_{txi-1/2j}}{\Delta x} + \frac{q^n_{tyij+1/2} - q^n_{tyij-1/2}}{\Delta y}\right\}$$

Parameterization for suspended and bedload sediment

The boundary condition given by equation (10) requires the values of sediment concentration at the reference level as a function of space and time. In general, the use of measurement data would be preferable for this purpose (Dang Huu and van Rijn, 2003). However, since these are very difficult to obtain, an empirical formulation is used instead, given by van Rijn (1984):

$$c_a = \frac{0.015 d_{90} T_s^{1.5}}{z_a D_*^{0.3}} \tag{20}$$

$$T_s = \frac{\tau_{0s} - \tau_{cr}}{\tau_{cr}}(\tau_{0s} > \tau_{cr}), D_* = \left[\frac{g(s-1)}{\upsilon^2}\right]^{1/3} d_{50},$$

$$s = \frac{\rho_s}{\rho_0}, z_a = \mathrm{Max}(0.01h, 0.5\Delta_s, 2.5d_{50})$$

$$\Delta_s = \begin{cases} 0, & \tau_{0s} < \tau_{cr} \text{ or } \tau_{0s} > 26\tau_{cr} \\ 0.11h(d_{50}/h)^{0.3}\left(1 - e^{-0.5T_s}\right)(25 - T_s), & \tau_{cr} < \tau_{0s} < 26\tau_{cr} \end{cases}$$

The bedload transport rate q_b is determined from the following expression (van Rijn, 1984):

$$\frac{q_b}{\sqrt{(s-1)gd_{50}^3}} = \begin{cases} m\left(|\theta| - \theta_{cr}\right)^n \Phi, & |\theta| \geq \theta_{cr} \\ 0, & \text{else} \end{cases}, \tag{21}$$

$$m = 5, n = 1.78, \Phi = \mathrm{sign}(\theta) \tag{22}$$

If bed slope effects are included explicitly, m, n and Φ are chosen as (Soulsby, 1997):

$$m = 6, n = 1.5, \Phi = \frac{\vec{\tau}}{|\vec{\tau}|} - k_* \nabla_{xy} z_b, k_* = \frac{1}{\tan\phi_r}\left(\frac{\theta_{cr}}{|\theta|}\right)^{0.5} \tag{23}$$

And the critical shear stress for a flat bed is corrected by a factor:

$$\theta_{cr} = \theta_{cr0}\left[1 + \frac{1}{\tan\phi_r}\frac{\vec{U}\cdot\nabla_{xy} z_b}{|\vec{U}|}\right] \tag{24}$$

Formula (24) is valid for bed slopes smaller than about 10^0. The critical Shields parameter for a flat bed, θ_{cr0}, is determined according to Soulsby and Whitehouse (Soulsby, 1997).

It should be noted that equations (20)-(24) are only one of specific formulae for calculation of sediment transport with or without bed slope correction. In general, they are quite often used in practice and the choice can be considered as a way of approach.

Simulations and discussion

The Sylt-Romo tidal bight (Figure 1) is located at the west coast of Schleswig-Holstein in northern Germany. The bight covers an area of approximately $20 \times 30\,\mathrm{km}^2$ and is characterized by shallow intertidal flats and deep tidal channels branching from the inlet into the interior of the bay (its bathymetry contours are shown in Figure 2). Water exchange with the sea can occur only through the tidal inlet. In the north and in the south, the bay is limited by dams. The tide is dominated by the M_2 component, and the tidal range is about 2.5 m. Close to the tidal channels, the sediment is made up primarily of non-cohesive sand with grain sizes between 150 and 300 μm. The rear areas of the bight are covered by fine sands and cohesive matter. The maximum water depth in the solution domain is about 30 m.

The solution domain is covered by a horizontal regular mesh with grid sizes $\Delta x = \Delta y = 100\,\mathrm{m}$, while the vertical grid spacing is 0.5 m resulting in about 2.7×10^6 active grid points. For the tidal forcing at the entrance of the bay, the time series of

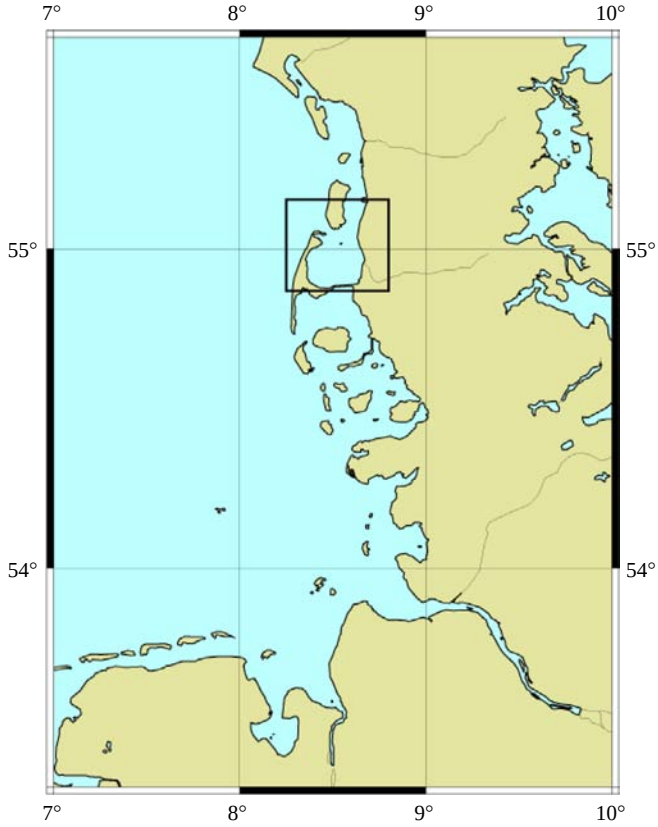

Figure 1.
Sylt-Romo bight, the area of computation

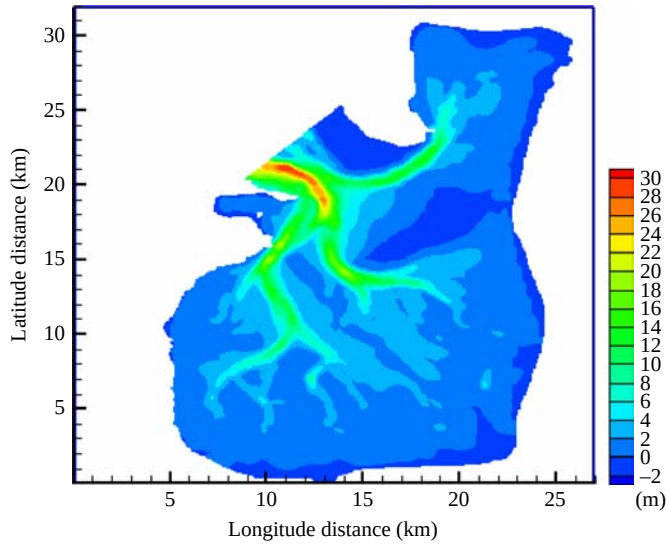

Figure 2.
Bathymetry contours of Sylt-Romo bight

water levels was taken from the tide gauge at Westerland/Sylt using a time lag of about half an hour. The time lag between the southern and northern entrance was neglected since the tidal wave length is large enough compared to the entrance diameter. Simulations were performed for different choices of parameters and boundary conditions (Table I). To avoid erosion and deposition due to dynamical imbalance, sediment transport is turned on after 20 h after the start of the simulation.

Case 1 is used as a reference run to which the other cases are compared. It includes the influence of bed slope correction, the hydrostatic pressure assumption, a mixed boundary condition at the lower boundary for suspended sand concentration, a coarse sand diameter of 300 μm, a sea water temperature of 18 °C and the last parameter is the salinity of 30 ppt.

Case 2 is different from Case 1 by excluding the effect of the bed slope correction through use of van Rijn's bedload transport formula. In Case 3, the pure Dirichlet boundary condition at the bottom for the suspended sand diffusion equation is used instead of the mixed boundary condition. The full non-hydrostatic pressure is taken into account in Case 4. Case 5 is for a smaller median grain size. The difference in the temperature is carried out by Case 6 and finally, Case 7 represents another option of salinity.

Case	Bed slope correction	Boundary kind	Non-hydrostatic pressure	d_{50}(μm)	Temperature (°C)	Salinity (ppt)
1	Yes	Mixed	No	300	18	30
2	No	Mixed	No	300	18	30
3	Yes	Dirichlet	No	300	18	30
4	Yes	Mixed	Yes	300	18	30
5	Yes	Mixed	No	160	18	30
6	Yes	Mixed	No	300	25	30
7	Yes	Mixed	No	300	18	35

Table I.
Different conditions for five computed cases

Figures 3-4 show the simulation result for Case 1. The water level contours and the velocity field near the surface at time $t = 150$ h are shown in Figure 3. This time step falls into an ebb-tide period (Figure 5), so the areas without flow velocity are very shallow (becomes dry) and at this time the water levels are still not updated. The current is flowing outwards to the open sea, where high velocities occur in the tidal channels reaching up to 1.6 m/s near the entrance of the bay. Consequently, sediment transport is high in these areas causing local erosion and deposition. The suspended

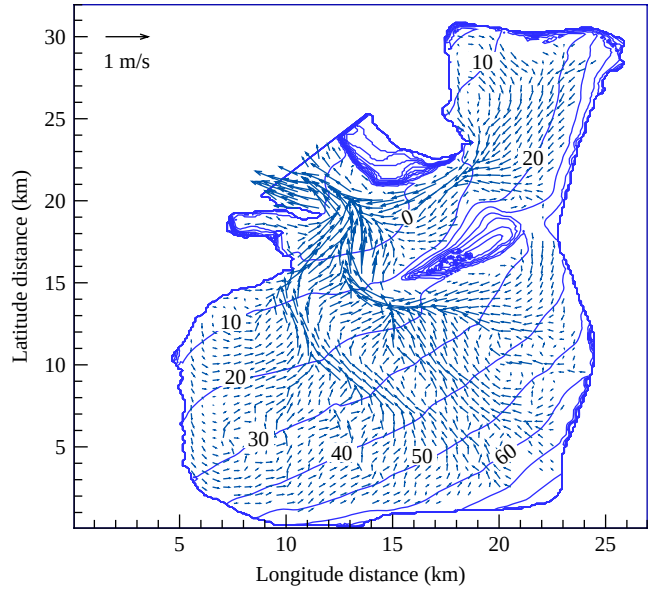

Figure 3.
Water level contours (in cm) and flow velocity field in the uppermost grid layer at $t = 150$ h

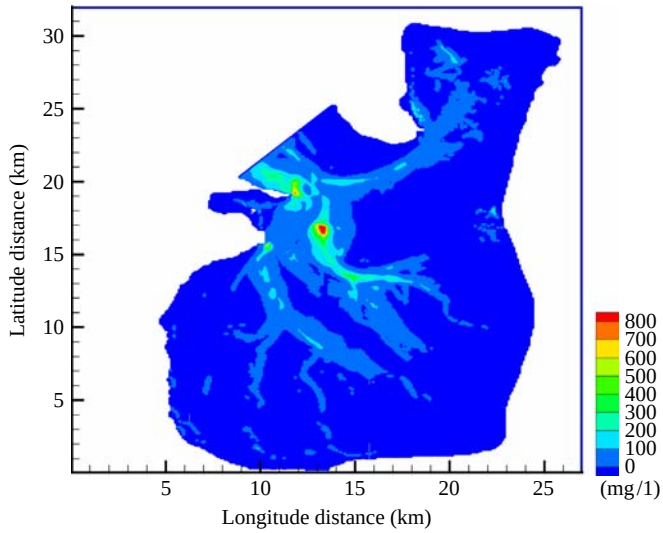

Figure 4.
Contours of suspended sand concentration near bed at $t = 150$ h

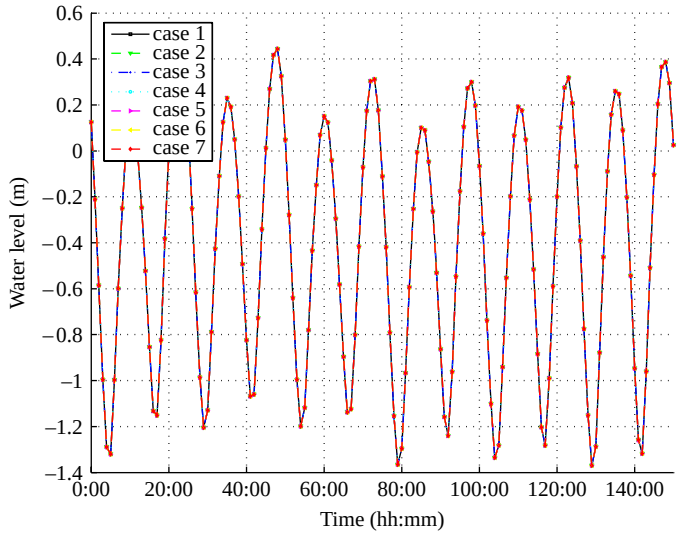

Figure 5.
Instantaneous water level at location (10.8, 15.6) km

sediment horizontal distribution near the bed is shown in Figure 4 showing a maximum value of more than 800 mg/l. It can be seen that sediment concentrations and transport rates are confined to the lowest layers.

This finding is corroborated by considering the profiles for the five cases at location (10.8, 15.6) km in Figure 6. The bed level at this location is about 15 m below MSL, however, suspended sand is confined to the lower 3 m, i.e. 1/5 of the water depth. Also, from Figure 6 it can be seen that Cases 1-4 and 7 give the same profiles, while Cases 5 and 6 is quite different. The distribution of concentration in Case 5 for fine sand is different from the others by higher sand concentrations in the upper layers, while the

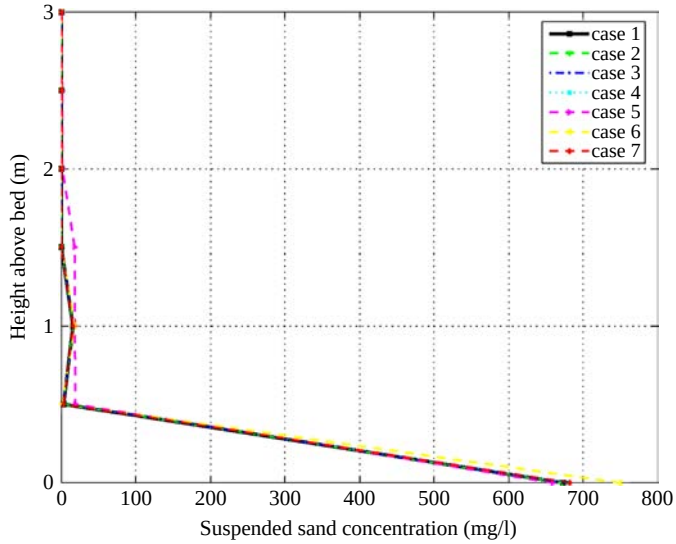

Figure 6.
Sand concentration profiles at location (10.8, 15.6) km at the time instant of peak value ($t = 146$ h)

distribution of Case 6 is concentrated in the lower and these are completely suitable to the practice. It means that the settling velocity of sand particle is directly proportional to the water temperature and the grain size. Figure 7 shows the time evolution of suspended sand concentrations at the same location near bed and it confirms again the suitability with the above comment for Figure 6. The scales of the components of sand transport rates can be observed in Figure 8 for Case 1 as a typical one and from there it is found that the general ratio between suspended transport and bedload transport is about 1/3. Figure 9 shows the rate of bed evolution versus time, in which it can be seen that only Case 5 is separate from Case 1, while the remainder seems undistinguishable. The explanation for this situation will be given later.

In order to draw the exact remarks, it requires a comprehensive evaluation for the whole area of computation. In general, at this location the bed evolution has a tendency of erosion and oscillation around a linear curve. Figure 10 shows an overall view on the status of erosion and deposition of the whole area of computation for Case 1. The range of bed level change is from -5 to 5 cm (positive value corresponding to erosion). It shows that the erosion and deposition mainly occur at the deep tidal channel, where the bed slope is quite large.

In order to give more detail on the sensitivity of bed morphologic process for each case under consideration, Figures 11-16 show more information on the discrepancies of bed level between Case 1 and case i ($\Delta = z_{b1} - z_{bi}, i = 2/7$) over 150 h, respectively. The range of discrepancy is divided into 6 levels distinguishing between positive and negative discrepancies as shown by the legends. From visual comparisons it is easy to see that the bed slope (Figure 11) really has a very strong influence on the process of bed morphology and the next factor is the grain size (Figure 14) that makes a considerable change in comparison with Case 1. Also from here, it is observed that the temperature of sea water (Figure 15) is a quite important parameter as discussed in the previous study by Dang Huu (2007). The impact of three remaining parameters

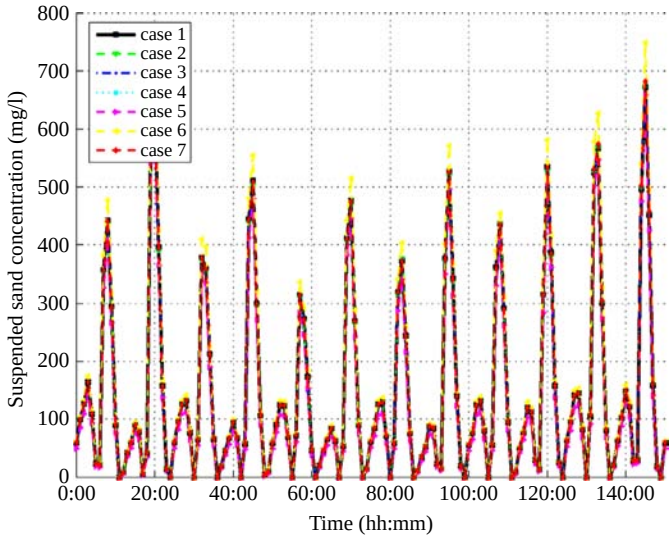

Figure 7.
Suspended sand concentrations near bed versus time at location (10.8, 15.6) km

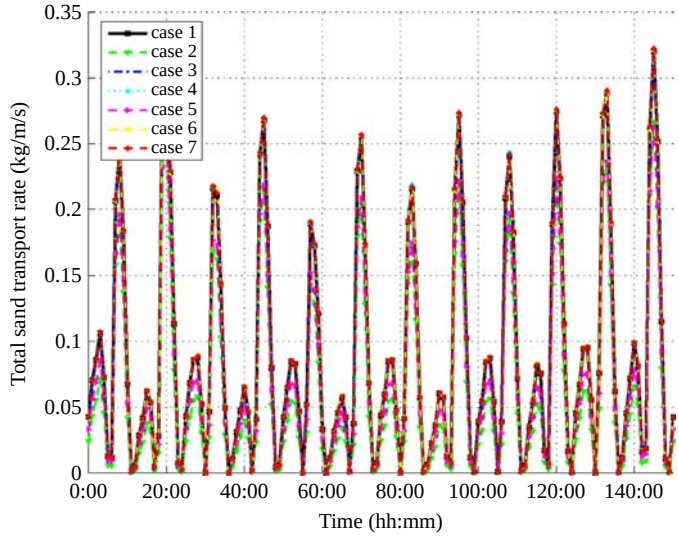

Figure 8.
Total sand transport rates versus time at location (10.8, 15.6) km

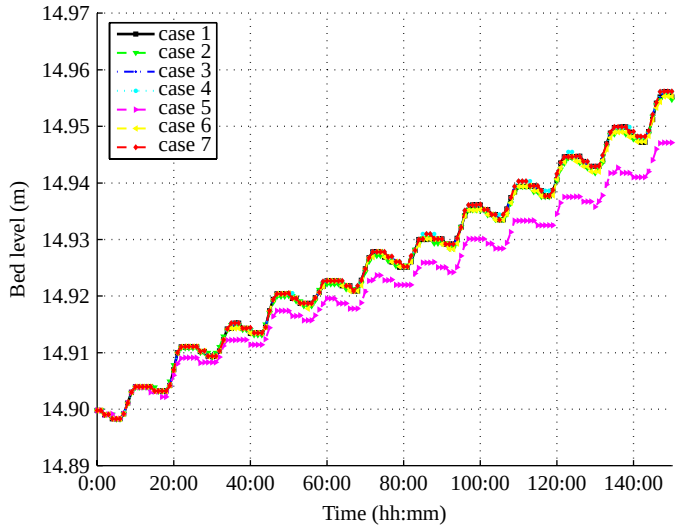

Figure 9.
Bed evolution in time at location (10.8, 15.6) km

(Cases 3, 4 and 7) are very feeble as shown in Figures 12, 13 and 15, respectively. On the basis of this overall observation, the situation shown in Figure 9 can be easily explained. The separation of the curve of Case 5 is due to the strong impact of grain size and the similar situation is also expected for Case 2. However, since the bed slope at the location under consideration is about -0.02, so the discrepancy due to bed slope correction created by equations (21)-(24) is quite small.

Finally, the bulk parameters after 150 h of simulation presented in Table II give the overall evaluations for the seven cases. They fully agree with the above comments,

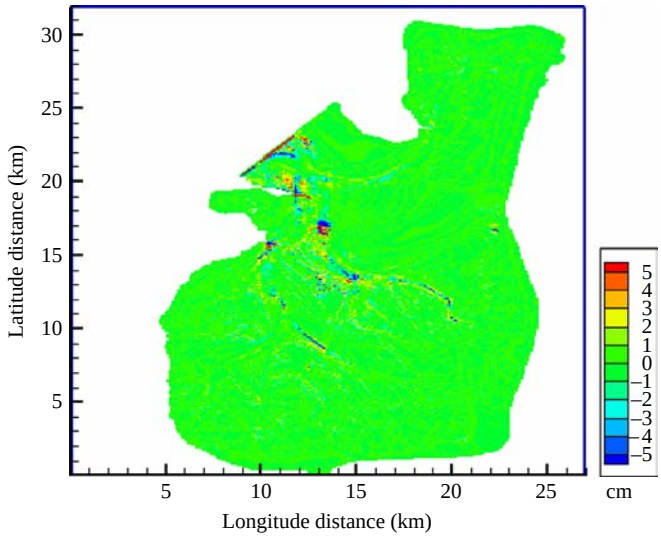

Figure 10.
Status of erosion (+) and deposition (−) after 150 h of Case 1

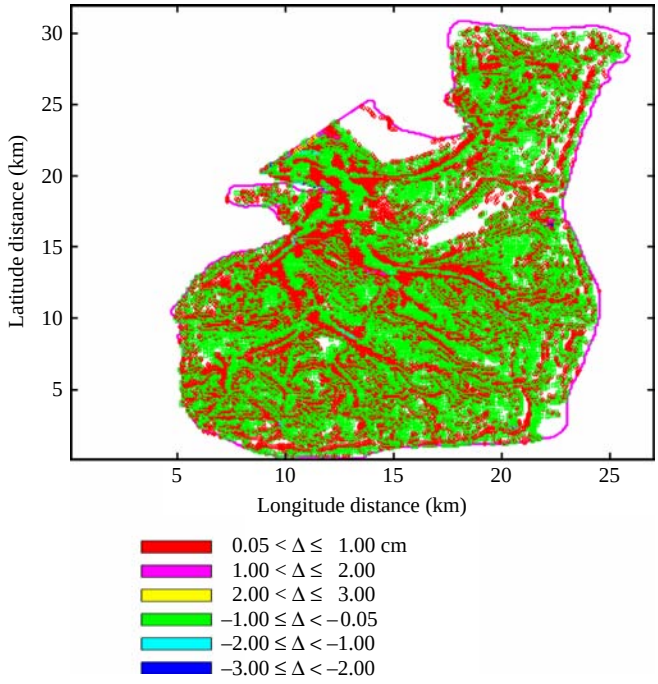

Figure 11.
Discrepancy of bed level between Cases 1 and 2 after 150 h

especially by the last column of Table II. This column provides the relative discrepancies of bed levels between Case 1 and the remainders in percentage of mean bed level change after 150 h of Case 1, in which Cases 2, 5 and 6 take approximately 31, 21 and 3 per cent, respectively.

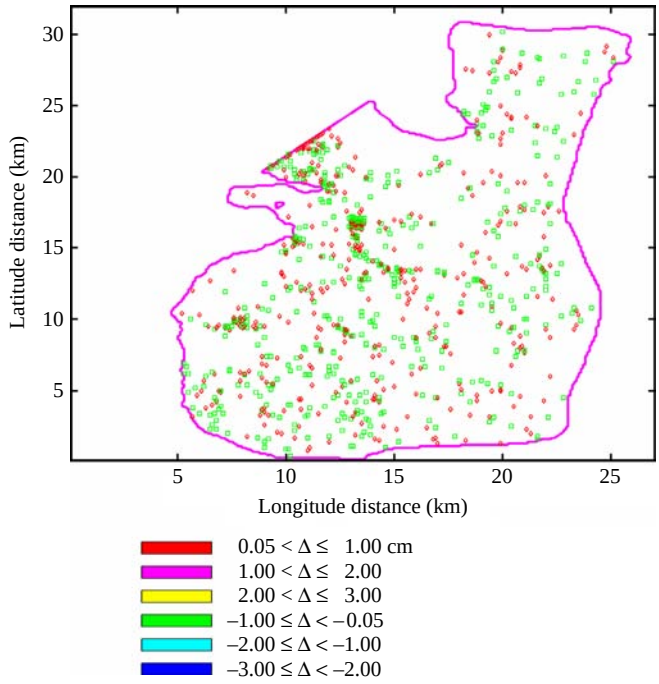

Figure 12.
Discrepancy of bed level between Cases 1 and 3 after 150 h

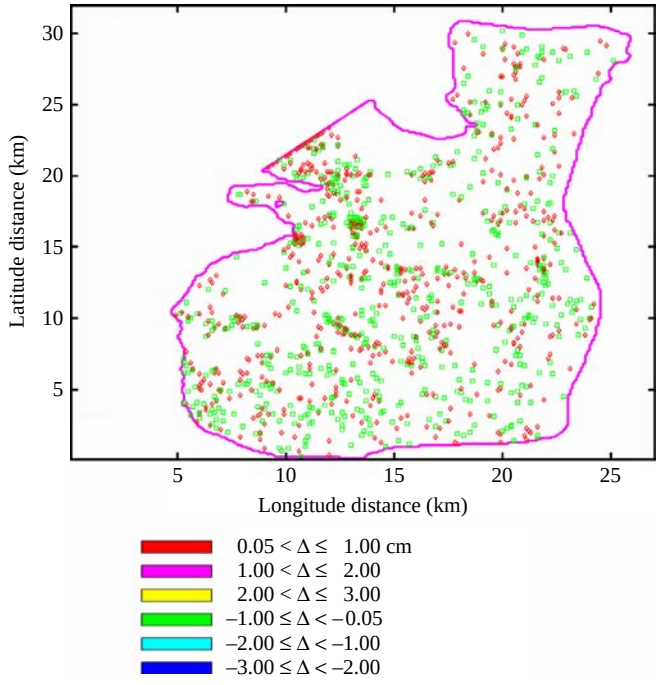

Figure 13.
Discrepancy of bed level between Cases 1 and 4 after 150 h

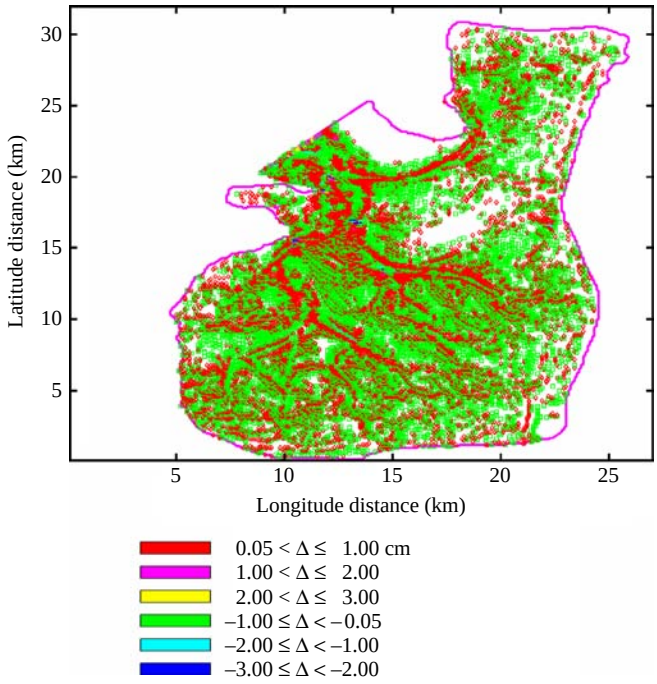

Figure 14.
Discrepancy of bed level between Cases 1 and 5 after 150 h

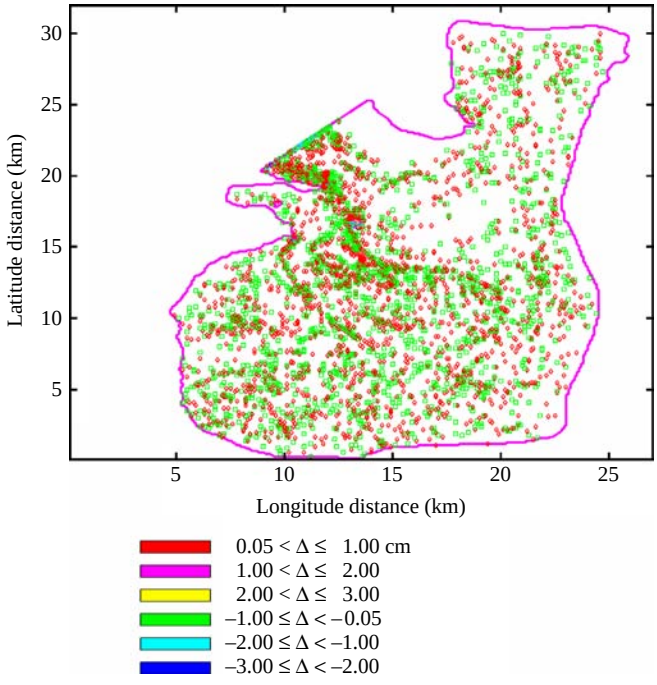

Figure 15.
Discrepancy of bed level between Cases 1 and 6 after 150 h

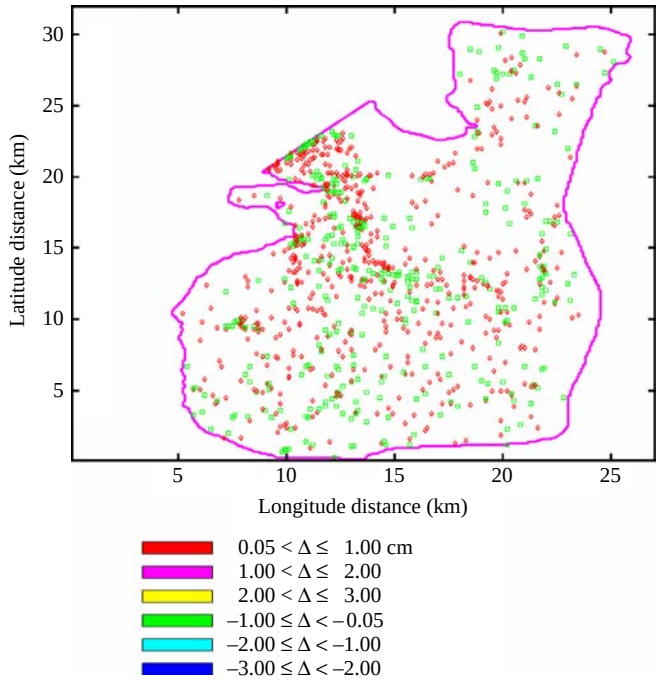

Figure 16.
Discrepancy of bed level between Cases 1 and 7 after 150 h

Case	V_{max} (m/s)	c_{max} (mg/l)	q_{tmax} (kg/m/s)	Δz_{bem} (cm)	Δz_{bdm} (cm)	$\Delta_m/\Delta z_{bm1}$ (per cent)
1	1.63	7,541	2.15	0.38	0.35	0
2	1.63	7,472	2.16	0.29	0.26	30.67
3	1.63	7,479	2.14	0.38	0.35	0.61
4	1.63	7,517	2.16	0.38	0.35	0.74
5	1.63	5,526	1.72	0.32	0.29	21.25
6	1.63	7,858	2.20	0.39	0.36	3.06
7	1.63	7,531	2.16	0.38	0.35	0.72

Table II.
Bulk parameters after 150 h of simulation

In general, the results of simulation have basically demonstrated the importance of seven given parameters, three of which are noticeable effective. Although the bed level change is small for this study, but it is believed that the deep area would be deformed by sedimentation in the long run.

Conclusions

A 3D hydrodynamical model, amended by a sediment transport module including suspended sediment and bedload transport together with bed update was applied to the Sylt-Romo bight. The sensitivity of sand transport and morphological changes to seven typical parameters (bed slope, kind of boundary condition, non-hydrostatic pressure term, sand grain size, sea water temperature and salinity) was investigated over a simulation time period of 150 h.

Based on the computed results the following conclusions are drawn:

- The influence of bed slope correction on bedload transport and consequently on the evolution process of bed morphology will become very strong, especially where the bathymetry has a large change. This will be more noticeable when the horizontal grid resolution is fine enough and therefore the bed slope is considered as a domimant factor within this study.
- The results of numerical simulation from using mixed versus Dirichlet boundary conditions are not really different. So, the difficulty of boundary condition treatment for finite difference method is removed. However, the sedimentation depends so much on the sand concentration at the reference level that is defined by an experimental formula.
- The affect of the non-hydrostatic pressure correction on the hydrodynamic field is quite small within this research. The extra amount of time to consume for this case is more than 50 per cent. It is known from experience that this term will really make sense when$(w/|\vec{V}|) \approx 1$. Therefore, in general, the assumption of hydrostatic pressure can be used to shorten the time of computation.
- The median diameter of sand particles plays an important role for bed evolution, especially for the vertical distribution of suspended sand concentration. Fine sand is easily picked up by the current to participate in suspension movement at higher layers of water column and then slowly settles on the bottom when the current velocity becomes small. This makes the sand concentration considerably decrease near bottom.
- The sea water temperature has a moderate impact on the distribution of sand concentration due to the increase of particle settling velocity, so the ability of sedimentation will be higher. Therefore, this factor should be paid more attention, especially in condition of global warming more and more.
- Bed morphology process seems less sensitive to the salinity within the range of value given. However, when the salinity considerably changes, the affect will appear at least for the vertical distribution of sand concentration by the way opposite to temperature.
- Finally, through the numerical simulation, the typical parameters related to sensitivity of morphological process have been basically examined. Such information will be interesting and useful for some problems of prediction or making some choices for an engineering project in practice.

References

Casulli, V. and Cattani, E. (1994), "Stability, accuracy and efficiency of a semi-implicit method for three-dimensional shallow water flow", *Computers Math. Applic*, Vol. 27 No. 4, pp. 99-112.

Casulli, V. and Stelling, G.S. (1998), "Numerical simulation of 3D quasi-hydrostatic, free-surface flows", *Journal of Hydraulic Engineering*, Vol. 124, pp. 678-98.

Chesher, T.J. *et al.* (1993), "A morphodynamic coastal area model", HR Wallingford, Report SR 337.

Chung, D.H. (2007), "Effects of temperature and salinity on the suspended sand transport", *International Journal of Numerical Methods for Heat & Fluid Flow*, Vol. 17 No. 5.

Chung, D.H. and van Rijn, L.C. (2003), "Diffusion approach for suspended sand transport under waves", *Journal of Coastal Research*, Vol. 19 No. 1, pp. 1-11.

Ezer, T. and Mellor, G.L. (2000), "Sensitivity studies with the North Atlantic sigma coordinate Princeton Ocean model", *Dynamics of Atmospheres and Oceans*, Vol. 32, pp. 185-208.

Kapitza, H. (2001), "TRIM documentation manual", GKSS Institute for Coastal Research, Report.

Mellor, G.L. and Ezer, T. (1995), "Sea level variations induced by heating and cooling: an evaluation of the Boussinesq approximation in ocean models", *Journal of Geophysical Research*, Vol. 100, C10, pp. 20.565-77.

Soulsby, R. (1997), *Dynamics of Marine Sands*, Thomas Telford Publications, London.

van Rijn, L.C. (1984), "Sediment transport. Part I: bed load transport. Part II: suspended load transport. Part III: bed forms and alluvial roughness", *J. Hydraul. Div., Proc. ASCE*, Vol. 110, HY10, pp. 1431-56; (HY11), pp. 1613-41; (HY12), pp. 1733-54.

Further reading

van Rijn, L.C. (1993), *Principles of Sediment Transport in Rivers, Estuaries and Coastal Seas*, Aqua Publications, Amsterdam.

van Rijn, L.C. (1998), *Principles of Coastal Morphology*, Aqua Publications, Amsterdam.

van Rijn, L.C. *et al.*, (1993), "Transport of fine sands by currents and waves I", *Journal of Waterway, Port, Coastal and ocean Engineering*, Vol. 119 No. 2, pp. 123-43.

Corresponding author

Dang Huu Chung can be contacted at: Dhchung@imech.ac.vn